Electronic Supplementary Material (ESI) for New Journal of Chemistry.

A Novel Gas Sensor Based on Porous α-$Ni(OH)_2$ Ultrathin Nanosheet/Reduced Graphene Oxide Composites for Room Temperature Detection of NO_x

Ying Yang[a,b], Hongjie Wang[a], Linlin Wang[a], Yunlong Ge[a], Kan Kan[a], Keying Shi[a] and Junhong Chen*[c]*

[a] Key Laboratory of Functional Inorganic Material Chemistry, Ministry of Education. Key Laboratory of Physical Chemistry, School of Chemistry and Material Science, Heilongjiang University, Harbin, 150080, P. R. China. E-mail: shikeying2008@163.com (Keying Shi); Fax: +86 4518667 3647; Tel: +86 451 8660 9141.

[b] Key Laboratory of Applied Chemistry and Nanotechnology at Universities of Jilin Province, Changchun University of Science and Technology, Changchun 130022, P. R. China.

[c] Department of Mechanical Engineering, University of Wisconsin-Milwaukee, 3200 North Cramer Street, Milwaukee, Wisconsin 53211, United States.

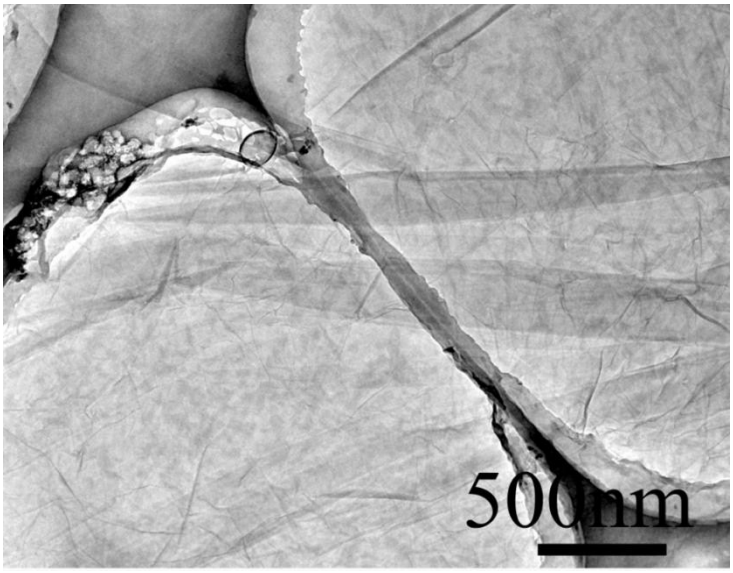

Figure S1. TEM image of the prepared GO by modified Hummers method.

Figure S1 shows the TEM image of the prepared GO by modified Hummers method. The GO is thin and transparent.

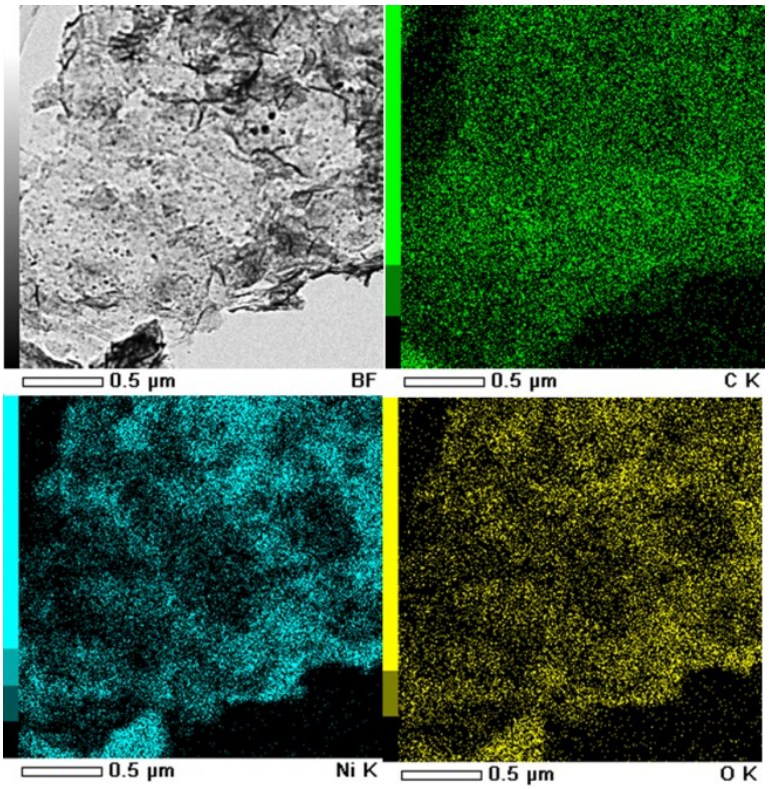

Figure S2. Elemental mapping of C2 sample: a) Bright field image; b), c) and d) corresponding C, Ni and O elemental mapping.

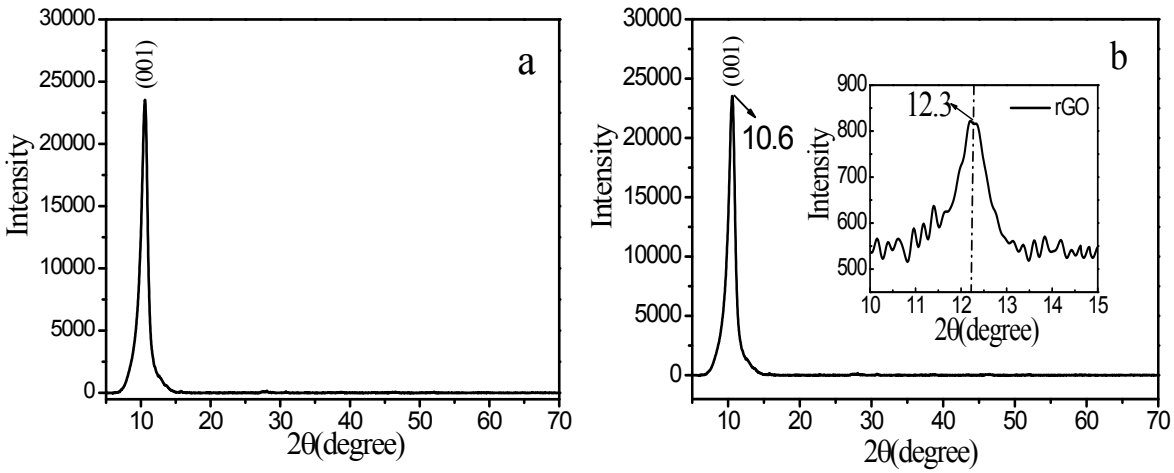

Figure S3. The XRD patterns of (a) the as-prepared GO by a modified Hummers method, and (b) the synthesized rGO obtained by reflux in the absence of the $Ni(NO_3)_2 \cdot 6H_2O$.

The weak diffraction peak at 2θ=12.2° can be indexed to the (001) plane of graphite oxide, and the

broad diffraction peak at 2θ of 24.5-27.5° can be indexed to the (002) planes of the graphite (G) in Figure. S3a. Figure. S3b shows the XRD pattern of the rGO. In Figure. S3b, the (001) peak of graphite oxide was greatly reduced, and the very broad (002) peak of graphite can be seen, suggesting that the graphite component is very poorly ordered along the stacking direction.

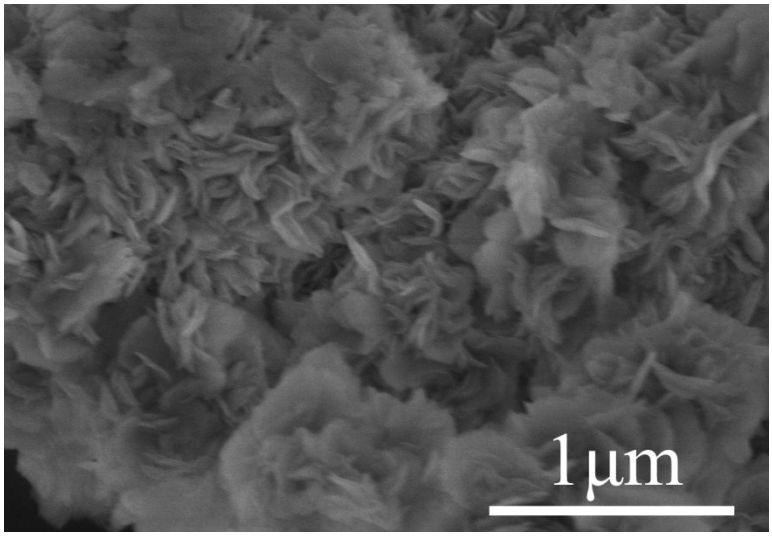

Figure S4. SEM image of the pure α-$Ni(OH)_2$ obtained by reflux.

Table S1. Data of sensitivity of α-$Ni(OH)_2$/rGO nanocomposites with different mass ratio of $Ni(NO_3)_2 \cdot H_2O$/GO exposed to NO_x with decreasing concentrations.

Concentration of NO_x ppm	S/% C1	S/% C2	S/% C3	S/% C4
97.0	29.3	64.4	50.0	12.4
68.1	22.8	61.5	44.5	11.3
48.5	19.0	56.5	41.0	10.0

29.1	17.0	49.1	33.9	8.6
9.7	11.8	40.7	28.6	6.7
4.85	9.0	31.0	23.5	--
2.91	6.7	23.2	17.8	--
0.97	4.3	16.5	11.2	--

Table S2. Data of response time of α-$Ni(OH)_2$/rGO nanocomposites with different mass ratio of $Ni(NO_3)_2 \cdot H_2O$/GO exposed to NO_x with decreasing concentrations.

Concentration of NO_x ppm	t/s C1	t/s C2	t/s C3	t/s C4
97.0	9	10	12	16
68.1	10	12	14	18
48.5	10	12	16	18
29.1	11	13	15	20
9.7	10	12	16	21
4.85	12	13	16	--
2.91	16	20	40	--
0.97	48	40	56	--

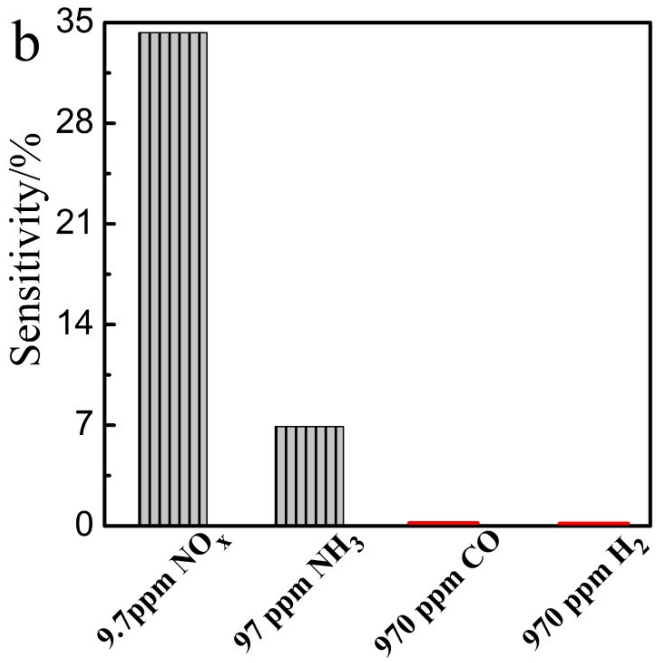

Figure S5. The bar graphs for gas selectivity of the C2 sensor to NO_x, NH_3, CO and H_2

Table S3. Fitted impedance parameters of samples

Samples	$R_\Omega(\Omega)$	C(F cm^{-2})	$R_{ct}(\Omega)$
α-$Ni(OH)_2$	579.5	5.57×10^{-6}	2.74×10^3
C2	772	1.91×10^{-6}	3.10×10^3
rGO	661.8	2.15×10^{-8}	0.26×10^3

The result of the impedance of the α-$Ni(OH)_2$, C2 and rGO electrodes are shown in Table S3. The results demonstrate that the C2 sample have the Rct of $3.10\times10^3\Omega$, which exhibits much higher conductivity than the pure α-$Ni(OH)_2$ sample. Therefore, the C2 sample can improve the electron transportation from the sensor to the adsorbate's NO_x surface, and consequently.